



Andean Geology

ISSN: 0718-7092

revgeologica@sernageomin.cl

Servicio Nacional de Geología y Minería  
Chile

Hervé, Francisco; Fanning, C. Mark

Late Triassic detrital zircons in meta-turbidites of the Chonos Metamorphic Complex, southern Chile

Andean Geology, vol. 28, núm. 1, julio, 2001, pp. 91-104

Servicio Nacional de Geología y Minería

Santiago, Chile

Available in: <http://www.redalyc.org/articulo.oa?id=173918535005>

- How to cite
- Complete issue
- More information about this article
- Journal's homepage in redalyc.org

redalyc.org

Scientific Information System

Network of Scientific Journals from Latin America, the Caribbean, Spain and Portugal

Non-profit academic project, developed under the open access initiative

## Late Triassic detrital zircons in meta-turbidites of the Chonos Metamorphic Complex, southern Chile

Francisco Hervé

Departamento de Geología, Universidad de Chile, Casilla 13518,  
Correo 21, Santiago, Chile  
fhervé@cec.uchile.cl

C. Mark Fanning

Research School of Earth Sciences, The Australian National University,  
Canberra, ACT 0200, Australia

### ABSTRACT

Sensitive High Resolution Ion MicroProbe (SHRIMP) U-Pb age determinations of detrital zircons from metasandstones of the Chonos Metamorphic Complex reveal a significant population of Late Triassic ages. One of the samples is immediately underlying the coquinaceous bed containing fossils which were initially identified as Late Silurian-Early Devonian, and more recently as Late Triassic faunas. The zircon data confirm the latter age as the depositional age of the fossil bearing rocks, excluding completely the possibility of a Paleozoic depositional age. Similar U-Pb detrital zircon ages are recorded in two other samples, one of which was collected in the vicinity of strata containing *Lima* sp., confirming that a Late Triassic depositional age is widespread in the Eastern belt of the Chonos Metamorphic Complex. However, in a fourth sample, the youngest detrital zircons are Carboniferous in age. Construction of the accretionary prism was thus active in the Late Triassic, and its metamorphism probably took place during the Jurassic, in contrast with a previously accepted Late Paleozoic age.

*Key words: Late Triassic, U-Pb ages, Chonos Metamorphic Complex, Southern Chile.*

### RESUMEN

**Circones detríticos del Triásico tardío en metaturbiditas del Complejo Metamórfico Chonos, sur de Chile.** Las edades U-Pb de circones detríticos, obtenidas con el SHRIMP en metareniscas del Complejo Metamórfico de Chonos, revelan una abundante población de circones con edades correspondientes al Triásico Superior. Una de las muestras proviene del estrato que se ubica inmediatamente bajo la capa coquinácea con fósiles que inicialmente otros autores asignaron al Silúrico Superior-Devónico Inferior, y recientemente al Triásico Superior. Las edades de circones detríticos concuerdan totalmente con esta última, y eliminan la posibilidad de una edad paleozoica de deposición de las rocas fosilíferas. Otras dos muestras, una de las cuales proviene de las vecindades de un estrato que contiene *Lima* sp., dan resultados similares, lo que indica que esta edad de deposición tiene amplia distribución en la franja oriental del Complejo Metamórfico de los Chonos. En cambio, en una cuarta muestra la edad más joven de circones detríticos es carbonífera. La construcción del prisma de acreción estaba activa en el Triásico Superior, y su metamorfismo tuvo lugar, probablemente, durante el Jurásico, contrariamente a la edad paleozoica superior que se le asignaba hasta ahora.

*Palabras claves: Triásico tardío, Edades U-Pb, Complejo Metamórfico Chonos, Sur de Chile.*

## INTRODUCTION

The Chonos Metamorphic Complex (CMC) is part of an accretionary complex which crops out as a continuous belt in the coastal area of Chile from Pichilemu (34°S) to the Taitao Peninsula (47°S), and discontinuously from there to the southernmost tip of South America.

The time frame proposed for the evolution of the low grade Chonos Metamorphic Complex (Davidson *et al.*, 1987), and for all the accretionary complex (*e.g.*, Hervé, 1988), has been strongly influenced by the identification by Miller and Sprechmann (1978) of a Late Silurian-Early Devonian fossil fauna in a coquinaceous metaturbidite bed in the southern end of Isla Patranca and in a small unnamed islet 5 km to the north. These fossiliferous localities, unique within the whole complex, were re-examined by Fang *et al.* (1998) who identified more recently collected fossil specimens as a Late Triassic *Monotis* species in Isla Patranca (named Potranca in Miller and Sprechmann, 1978) and *Lima* sp., of a Permian to Triassic age range.

The Chonos Metamorphic Complex has been studied previously by Miller (1979) and Hervé *et al.* (1981). Detailed field and structural studies led Miller (1979) to recognize three stratigraphic units, the Canal King, Potranca and Canal Pérez Sur informal formations, interpreted to be progressively younger successions, separated by unconformities. However, the three units share a common structural grain, characterized by northwest trending fold axes and stretching lineations. The fossil assemblages noted above occur in the middle Potranca formation, which was assigned to the Late Silurian-Early Devonian. It follows that the underlying Canal King formation is older and that the overlying Canal Pérez Sur formation is younger.

In an alternative view, Hervé *et al.* (1981) distinguishes an Eastern belt\* where primary sedimentary structures are preserved, which grades into a Western belt where all primary structures have been lost due to increasing deformation and metamorphism. This interpretation is based on both structural continuity and a progressive increase in metamorphic grade from one belt to the other. The Eastern belt is considered to have a Devonian protholith, and be composed of the Patranca facies and the Teresa facies, roughly equivalent to the Potranca and Canal Pérez Sur formations of Miller (1979), respectively. Davidson *et al.* (1987) presented Rb-Sr whole rock ages of ca. 220 Ma on slates from the Eastern belt which were interpreted as the age of the D2 metamorphic episode in the complex. They presented Rb-Sr errorchron data on the schists from the Western belt of ca. 140 Ma and ca. 168 Ma which they interpreted as indicating a Jurassic 'reactivation' of the subduction complex.

Willner *et al.* (2000) have shown that the metamorphism within the Eastern belt of the Chonos Metamorphic Complex took place under peak P-T conditions of 5.5 Kbar and 250-280°C and 8-10 Kbar and 380-500°C in the Western belt. These rather high P-T gradients are in accordance with a subduction zone environment of metamorphism.

The purpose of this paper is to present the results of SHRIMP U-Pb age determinations for detrital zircons from rocks of the fossiliferous unit. These results elucidate the contradiction between the two previously published paleontological age interpretations and they establish constraints on the age of deposition and metamorphism of the Potranca formation in the Chonos Metamorphic Complex.

## SAMPLES AND METHODOLOGY

Three metasedimentary rock samples of the turbiditic unit (Potranca formation or Patranca facies of the Eastern belt) which contain the fossiliferous strata in the Chonos Metamorphic Complex

were collected for U-Th-Pb dating of zircon by SHRIMP (Sensitive High Resolution Ion MicroProbe) at The Australian National University. An additional metasedimentary rock from the Teresa facies (Ca-

\* The terms Eastern and Western belts as used here should not be confused with the terms Western and Eastern Series, terminology that has been the formal nomenclature since Aguirre *et al.* (1972), used with the accretionary complex north of Chiloé and more recently by Martín *et al.* (1999), for rocks found between 38 and 41°S.

nal Pérez Sur formation) was also analysed. Zircons were separated using standard crushing, heavy liquid and Frantz isodynamic methods. Grains from the total zircon population were sprinkled onto double sided tape and cast in an epoxy disk together with the Duluth Gabbro reference zircon, AS3 (see Paces and Miller, 1993). The ion microprobe procedures used essentially follow those given in Compston *et al.* (1992) and Williams (1998). The U/Pb ratios have been calibrated relative to the AS3 zircons, which have an age of 1099 Ma (Paces and Miller, 1993). One spot was analyzed in each crystal, unless specified in the tables by a number of the form n.2, usually in the outer rim.

The age spectra of individual rock units can be used to obtain an inferred maximum depositional age of the original sediments; the depositional age can be no older than the youngest concordant U-Pb zircon age. Where a number of analyses (from different grains) have the same radiogenic  $^{206}\text{Pb}/^{238}\text{U}$  ratios to within analytical uncertainty, weighted mean ages have been calculated and those are reported, with uncertainties given at the 95% confidence level.

All samples analysed belong to the Eastern Belt of the Chonos Metamorphic Complex. Their location is indicated in figure 1.

CE9603 is a metasandstone with L-tectonite fabric reflecting the intersection of two cleavages in northwest direction. It was collected from a turbidite succession devoid of fossils.

FO9606 is a medium grained metasandstone with convolute bedding. It was collected near the

southern end of Isla Patranca, from an horizon immediately underlying the coarse grained fossil bearing coquinaceous bed from which Miller and Sprechman (1978) and Fang *et al.* (1998) have identified Late Silurian-Early Devonian and Late Triassic fossils respectively. The coquinaceous bed from this location shows clear indications of having previously been sampled. The authors, therefore, believe that this coquinaceous bed was sampled to produce the Miller and Sprechman (1978) fossils, and the authors know with absolute certainty that this is the location described in Fang *et al.* (1998) since the material was collected by the senior author. The contact between the metasandstone sampled for this U-Pb zircon study and the coquinaceous bed used for the fossil age determinations is of normal conformable sedimentary nature.

CE9625 is a low grade fine grained metaconglomerate collected in the islet where *Lima* sp. was identified by Fang *et al.* (1998). Continuous slate beds form only 5% of the succession, which is mainly composed here by turbidites with sole marks, dewatering structures, convolute bedding and rip clasts of shale. The rocks are cleaved and have a northwest lineation.

FO9640 is a fine grained metasandstone from the southeastern corner of Isla Yechica, where an inverted succession of turbidites with interbedded banded cherts crops out. Beds are typically 0.5 m thick, bioturbated, and with a subhorizontal tectonic lamination, axial planar to ENE folds of the stratification.

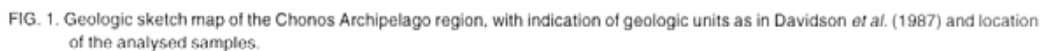
## GEOCHRONOLOGICAL RESULTS

The SHRIMP U-Pb detrital zircon results for the samples CE9603, FO9606 and CE9625 (Patranca facies or Potranca formation) are presented in tables 1-4, p. 101-104. The results for sample FO9640 (Teresa facies or Canal Pérez Sur formation) are presented in table 4. The data are shown on the Tera-Wasserburg diagrams in figure 2, and on relative probability plots in figure 3, respectively.

The three samples of the Potranca facies record similar results, with a wide range of ages. The age spectra are complex revealing multiple source provenance for the detrital zircon grains.

However, some common aspects between the samples can be highlighted:

- Most of the zircons are igneous in origin, they have euhedral to subhedral outlines and cathodoluminescence (CL) images of the sectioned grains show well developed, simple magmatic zoning.
- The youngest zircon analysis in each sample, with isotopic ratios plotting within uncertainty of the Tera-Wasserburg concordia, are ca. 210 Ma (212, 216 and 208 Ma, respectively). There are few analyses which are younger, however these are discordant and so the ages are not considered to



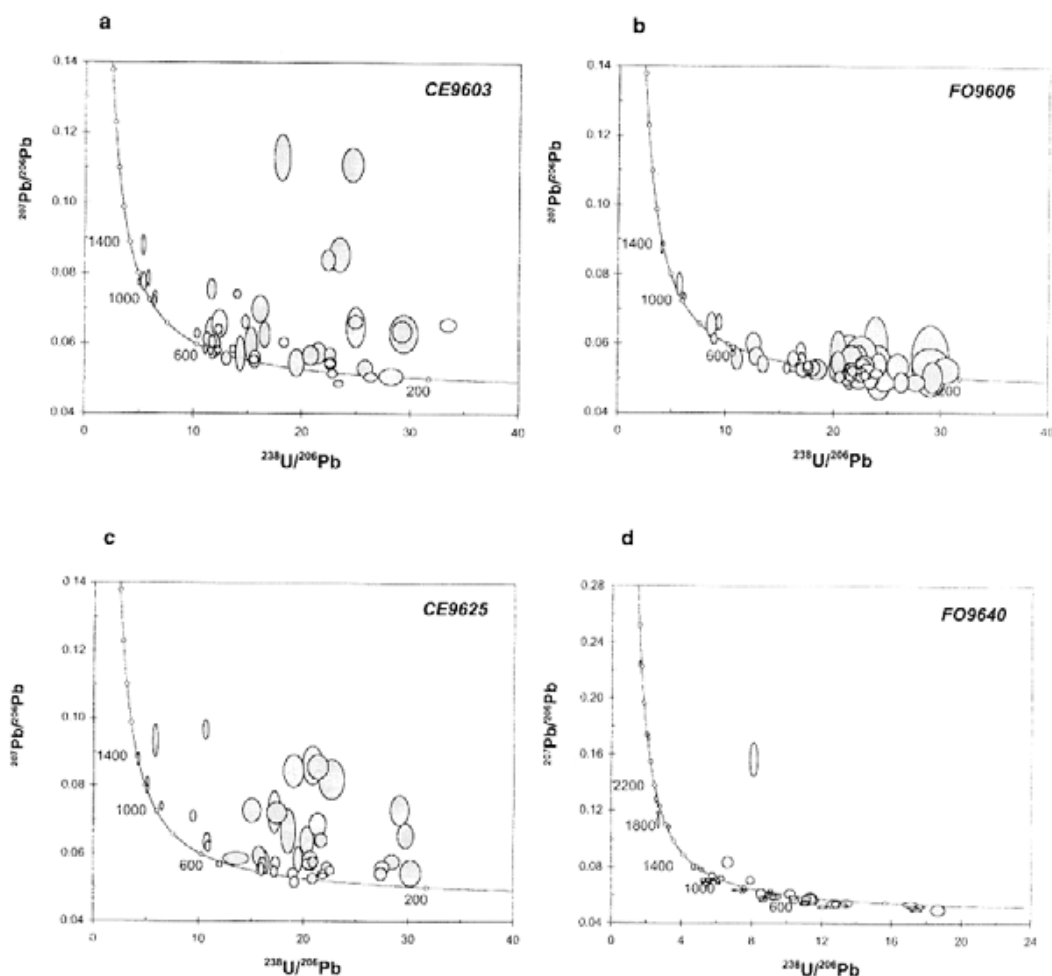


FIG. 2. Tera and Wasserburg (1972) concordia diagrams for **a**- sample CE9603; **b**- sample FO9606; **c**- sample CE9625, and **d**- sample CE9640. The calibrated  $^{238}\text{U}/^{206}\text{Pb}$  ratios versus the total  $^{207}\text{Pb}/^{206}\text{Pb}$  ratios have been plotted as one sigma error ellipses. Note that an analysis that is not within uncertainty of the concordia curve may not necessarily signify a discordant analysis. It may simply reflect that a significant amount of common Pb has been detected in that analysis. The U/Pb isotopic data are given in the tables as both uncorrected and  $^{207}\text{Pb}$  corrected radiogenic ratios (see Compston *et al.*, 1992).

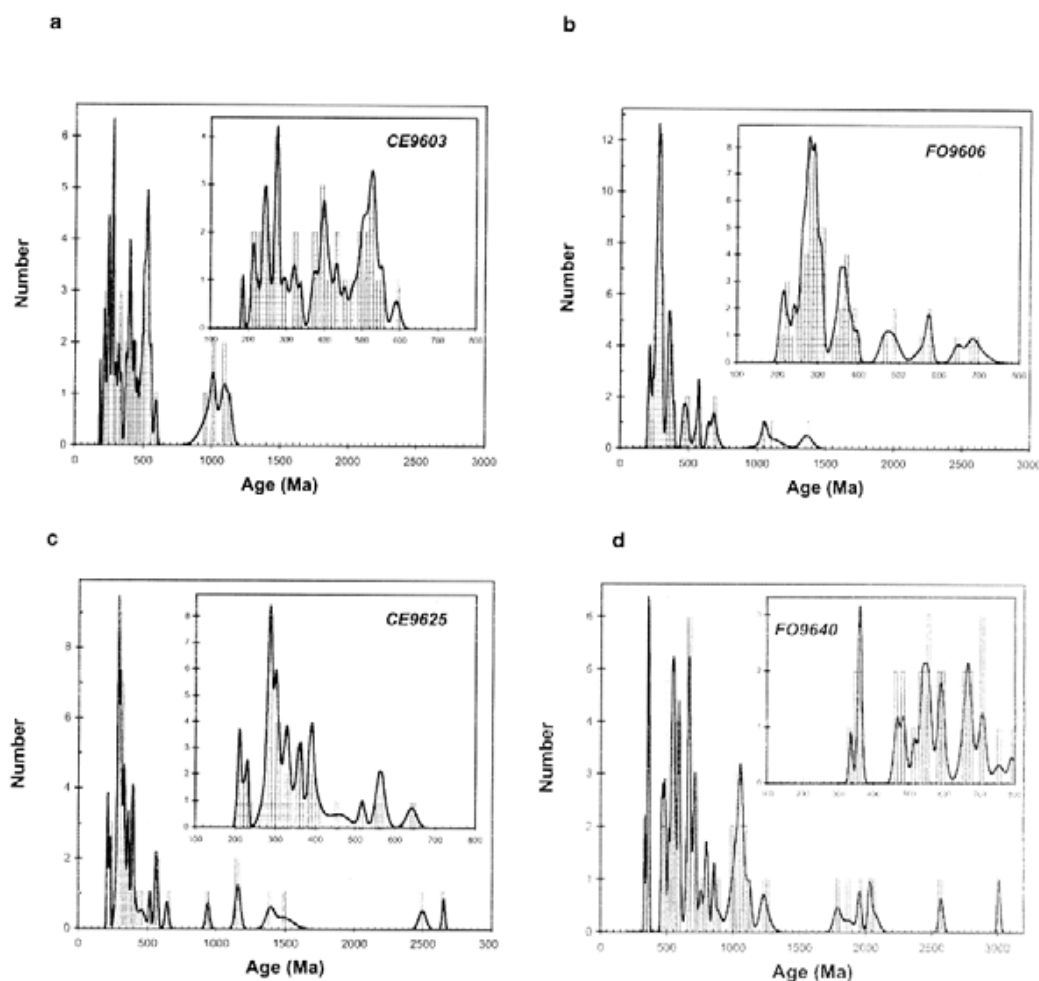


FIG. 3. Age versus probability diagrams for **a**- sample CE9603; **b**- sample FO9606; **c**- sample CE9625, and **d**- sample FO9640. The relative probability curve takes into account the age and age uncertainty for each analysis. The stacked histogram indicates the number of analyses that contribute to the various peaks in the relative probability curve.

necessarily represent the time of crystallisation of the zircons. The youngest concordant ages form a grouping at ca. 220 Ma in all three samples.

- Most (>80%) of the zircons analysed are Paleozoic in age, and they show a complex distribution with age peaks (Figs. 1b, 2b, 3b) at ca. 280 Ma, at 330-350 Ma, at 400 Ma, with very few zircons between 400 and 530 Ma, and a further peak at ca. 550 Ma.

- Proterozoic zircons are scarce, they are mainly concentrated in the 1300-1600 Ma age range, and

are absent at  $800 \pm 50$  Ma.

- Only two Late Archean and/or Paleoproterozoic zircons are present in one of the samples.

The results for sample FO9640 (from the Teresa facies or Canal Pérez Sur formation) differ quite substantially from the above. The younger date for detrital zircons in this sample is  $336 \pm 5$  Ma (Early Carboniferous), and the proportion of Proterozoic grains is larger than in the three previous samples. Two Archean grains are present.

## DISCUSSION AND CONCLUSIONS

The U-Pb SHRIMP zircon age data obtained in this study strongly support the Late Triassic (Late Norian) depositional age determination made by Fang *et al.* (1998) based on the study of fossils in the Chonos Metamorphic Complex, and is in contradiction with the previously proposed Late Silurian-Early Devonian age by Miller and Sprechmann (1978). The fact that three samples from the same unit (the Potranca formation or Patranca facies) of the Chonos Metamorphic Complex show similar minimum ages indicates that the Late Triassic rocks are extensive and not simply restricted to the fossiliferous localities.

The coincidence between the radioisotopic zircon ages and the biostratigraphic depositional ages (Gradstein and Ogg, 1996) is remarkable, and probably indicates that active magmatism was occurring in the provenance area of the turbidite sequence during their deposition.

This provenance area is almost instinctively looked for in Patagonia, to the east of the analysed samples. However, in the Chilean slope of the Andes, igneous rocks of Late Triassic age are not known. A few granitic bodies of Late Triassic age do exist in the North Patagonian Massif (Cingolani *et al.*, 1992), hundreds of kilometers inland from the location of the Chonos Archipelago. A Carboniferous magmatic arc in the Lake District of Chile, was

exhumated and eroded previously to the Late Triassic (Martin, 1999). Also, the Mesoproterozoic and Late Proterozoic zircons, might have come from the presently covered basement of Patagonia, or they may be far travelled grains coming from the Namaquan belts of southern Africa, which was side by side to Patagonia in the Late Triassic.

Another possible source area for the detrital material is the Antarctic Peninsula (Fig. 4), whose exact position in the Early Mesozoic is not well known, but that in recent paleogeographic reconstructions, is located with its northern tip near the present latitude of the Golfo de Penas (47°S) (Lawver *et al.*, 1998). Turbidites of Norian age in the Trinity Peninsula Group occur near the northern tip of the Antarctic peninsula interbedded with acid volcanic rocks in the Legoupil Formation (Thomson, 1975). Early Triassic turbidites occur in the Myers Bluff Formation of Livingston Island (Willan *et al.*, 1994). Various detrital zircon age population diagrams have been published by Löske *et al.* (1985) which give strong evidence for Carboniferous and Late Proterozoic source regions.

The confirmation of the Late Triassic depositional age for at least a significant part of the Chonos Metamorphic Complex, implies that its metamorphism took place during the Mesozoic or Cenozoic. However, this metamorphism was probably Jurassic,

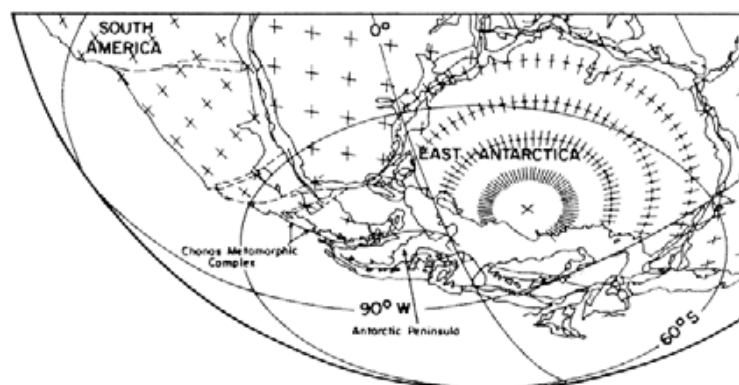


FIG. 4. Part of the tight fit paleogeographic reconstruction of Gondwana at 200 Ma (after Lawver *et al.*, 1998), showing that the present location of the Chonos Metamorphic Complex is just north of the tip of the Antarctic Peninsula in the Triassic-Jurassic boundary times.



as the Chonos Metamorphic Complex was intruded by the Early Cretaceous components of the North Patagonian Batholith (Pankhurst *et al.*, 1999), when it had already acquired its main structural characteristics. Also, Thomson *et al.* (2000) combining some of the SHRIMP data presented here and Fission Track age determinations conclude that the metamorphism in the CMC took place in the Early Jurassic. This allows a more confident interpretation of the Late Triassic to Jurassic Rb-Sr age data on rocks of the same unit (*in* Hervé, 1988) as related to the metamorphism or Early diagenesis of the complex.

However, the structurally homogeneous rock units within this metamorphic complex are not necessarily time-restricted depositional units. For example, the metaturbidite from the Teresa facies (Davidson *et al.*, 1987) of the Eastern Belt has given a detrital zircon age spectra which differs from those of the Patranca facies, in that the younger concordant zircon is 336 Ma, and the age *versus* probability pattern is different. They may represent older deposits.

The geographic and lithologic continuity of the Chonos Metamorphic Complex with the Paleozoic Metamorphic Complex of the Coastal Range of southcentral Chile and of the Chiloé island must now be considered carefully. The consequences of the data presented herein lead to significant changes in the interpreted age of deposition and metamorphism of the so-called Paleozoic basement rocks that previously had been considered on the basis of lithological (structural and metamorphic) criteria to form a simple single 'basement' package. Recent work by Duhart *et al.* (1997, 1999); and by Martin *et al.* (1999) in the Lake district of southern Chile, have documented that the Western Series of the paleozoic metamorphic basement includes sedimentary components younger than Early Permian. These same authors indicated that a regional cooling between 220 and 250 Ma is registered in the metamorphic complex, and that it took place after the main deformation and metamorphic event. Söllner *et al.* (2000) reported the presence of Late Carboniferous-Early Permian acid volcanic rocks in the 'basement' near Puerto Montt.

The Late Triassic turbidites of the Chonos Metamorphic complex dated here, are time equivalent to the Panguipulli Formation of the lake district, but the latter, which sits unconformably over the

metamorphic basement, has not experienced the high P/T metamorphism recorded in the CMC. So, the studied rocks were involved in deep subduction during the Late Triassic-Early Jurassic, which took place beneath the western continental margin of Gondwana while the Panguipulli rocks remained on the upper plate near the surface. In the Lake Region, Martin *et al.* (1999) suggested that the Western Series and the Late Carboniferous magmatic arc were exposed after the middle Permian to Middle Triassic exhumation and that initial transpressional deformation of the subduction-arc complex associated with an event of dextral oblique convergence along the margin took place during the Late Triassic-Early Jurassic. This scenario is based on structural observations on the rocks of the Western Series, and on previous paleomagnetic studies (Forsythe *et al.*, 1987) indicating northward translation of portions of the Coast Range, now situated near 30°S during Late Triassic to Late Jurassic. It is interesting to note here that starting in the Early Jurassic, the Antarctic Peninsula migrated southward, with a sinistral movement along the margin of Gondwana after the paleogeographic reconstructions (Scotese, 1997). The Chonos area is thus a portion of the margin where continental margin parallel strike slip movements during the Late Triassic to Early Jurassic seem to diverge, in a way similar to what would be expected when the subduction of a rise or indenter, beneath the continental margin occurs.

The oblique subduction which occurred in the area (Martin *et al.*, 1999) during the Late Triassic-Early Jurassic, together with a low subduction angle, could have resulted in the paucity of the production of magmatic rocks observed during this interval. The most conspicuous contemporaneous arc-like igneous complex is the Sub-cordilleran batholith (Haller *et al.*, 1999) in the eastern slope of the present Andes, which might be genetically related to the subduction event giving rise to the Chonos Metamorphic Complex.

It seems clear that the metamorphic basement of southern Chile certainly includes rocks varying widely in ages of deposition and metamorphism, which otherwise are very similar in structure and metamorphic mineralogy. Precise dating of deposition and metamorphism is a needed basis for understanding its evolution.

## ACKNOWLEDGEMENTS

Professor H. Miller (University of München) generously indicated the precise location of the fossil bearing localities he discovered in the 70's, which would have been impossible to relocate otherwise in the maze of islands which compose the Chonos Archipelago. R.J. Pankhurst (British Antarctic Survey), A. Demant (Université d'Aix-Marseille III), A. Willner (Ruhr Universität), H. Massone (Stuttgart Universität), C. Pimpirev

(Bulgarian Antarctic Institute) and V. Muñoz (Universidad de Chile) collaborated in the field work. Thorough reviews by H. Miller (München University), M. Martin (Massachusetts Institute of Technology) and U. Cordani (Universidad de Sao Paulo) helped to improve the manuscript. This study was funded by Fondecyt Projects 1980741/1010412 and Cátedra Presidencial de Ciencias to FH. It is a contribution to IGCP Project 436 'Pacific Gondwana Margin'.

## REFERENCES

- Aguirre, L., Hervé, F.; Godoy, E. 1972. Distribution of metamorphic facies in Chile, an outline. *Krystalinikum*, Vol. 9, p. 7-19.
- Cingolani, C.; Dalla Salda, L.; Hervé, F.; Munizaga, F.; Pankhurst, R.J.; Parada, M.A.; Rapela, C.W. 1992. Evolution of the North Patagonia Andes and the adjacent continental massif: new impressions of Andean and Pre-Andean Tectonics. In *Andean Magmatism and its tectonic setting* (Harmon, R.; Rapela, C.W.; editors). *Geological Society of America, Special Paper* 265, p. 29-44.
- Compston, W.; Williams, I.S.; Kirschvink, J.L.; Zhang Zichau.; Ma Guogan. 1992. Zircon U-Pb ages for the Early Cambrian time-scale. *Journal of the Geological Society of London*, Vol. 149, p. 171-184.
- Davidson, J.; Mpodozis, C.; Godoy, E.; Hervé, F.; Pankhurst, R.J.; Brook, M. 1987. Late Paleozoic accretionary complexes on the Gondwana margin of Southern Chile: evidence from the Chonos Archipelago. In *Gondwana Six: Structure, Tectonics and Geophysics* (McKenzie, G.D.; editor). *Geophysical Monograph*, 40, p. 221-227.
- Duhart, P.; Martin, M.; Muñoz, J.; Crignola, P.; McDonough, M. 1997. Acerca de la edad del protolito del basamento metamórfico de la Cordillera de la Costa de la X Región. Edades preliminares  $^{207}\text{Pb}/^{206}\text{Pb}$  en circones detriticos. In *Congreso Geológico Chileno*, No. 8, Actas, Vol. 2 p. 1267-1270. Antofagasta.
- Duhart, P.; Muñoz, J.; McDonough, M.; Martin, M.; Villeneuve, M. 1999.  $^{207}\text{Pb}/^{206}\text{Pb}$  and  $^{40}\text{Ar}/^{39}\text{Ar}$  geochronology of the coastal metamorphic belt between 41°-42°S in central-south Chile. In *International Symposium on Andean Geodynamics*, No. 4, *Extended Abstracts Volume*, p. 219-223. Göttingen.
- Fang, Z.; Boucot, A.; Covacevich, V.; Hervé, F. 1998. Late Triassic fossils in the Chonos Metamorphic Complex, southern Chile. *Revista Geológica de Chile*, Vol. 25, No. 2, p. 165-173.
- Forsythe, R.D.; Kent, D.V.; Mpodozis, C.; Davidson, J. 1987. Paleomagnetism of Permian and Triassic rocks in the central Chilean Andes. In *Gondwana Six: Structure, Tectonics and Geophysics* (McKenzie, G.D.; editor). *Geophysical Monograph*, 40, p. 241-252.
- Gradstein, F.; Ogg, J. 1996. A Phanerozoic time scale. *Episodes*, Vol. 19, No. 1-2, p. 3-5.
- Haller, M.J.; Linares, E.; Ostera, H.A. 1999. Petrology and geochronology of the subcordilleran plutonic belt of Patagonia. In *South American Symposium on Isotope Geology*, No. 2, Actas, Servicio Geológico Minero Argentino, Anales 34, p. 210-214. Buenos Aires.
- Hervé, F. 1988. Late Paleozoic subduction and accretion in Southern Chile. *Episodes*, Vol. 11, p. 183-188.
- Hervé, F.; Mpodozis, C.; Davidson, J.; Godoy, E. 1981. Observaciones estructurales y petrográficas en el basamento metamórfico del Archipiélago de los Chonos entre el Canal King y el Canal Ninualac. Aisen. *Revista Geológica de Chile*, No. 13-14, p. 3-16.
- Lawver, L.A.; Dalziel, I.W.D.; Gahagan, L.M. 1998. A tight fit Early Mesozoic Gondwana, a plate reconstruction perspective. *Memoirs of the National Institute for Polar Research*, Special issue, Vol. 53, p. 214-229. Tokio.
- Löske, W.; Miller, H.; Kramm, U. 1988. U-Pb systematics of detrital zircons from low grade metamorphic sandstones of the Trinity Peninsula Group (Antarctica). *Journal of South American Earth Sciences*, Vol. 1, No. 3, p. 301-307.
- Martin, M.; Kato, T.; Rodríguez, C.; Godoy, E.; Duhart, P.; McDonough, M.; Campos, A. 1999. Evolution of Late Paleozoic accretionary complex and overlying forearc-magmatic arc south-central Chile (38-41°S): constraints for the tectonic setting along the south-

- western margin of Gondwana. *Tectonics*, Vol. 12, No. 4, p. 582-605.
- Miller, H. 1979. Das Grundgebirge der Anden in Chonos-Archipel, Region Aisén, Chile. *Geologische Rundschau*, Vol. 68, No. 2, p. 428-456.
- Miller, H.; Sprechmann, P. 1978. Eine devonische Fannula aus dem Chonos-Archipel, Region Aisén, Chile und ihre stratigraphische Bedeutung. *Geologische Jahrbuch*, Vol. B28, p. 37-45.
- Paces, J.B.; Miller, J.D. 1993. Precise U-Pb ages of Duluth Complex and related mafic intrusions, north-eastern Minnesota: Geochronological insights to physical, petrogenetic, paleomagnetic, and tectono-magmatic process associated with the 1.1 Ga Mid-continent Rift System. *Journal of Geophysical Research*, Vol. 98, No. 13, p. 13997-14013.
- Pankhurst, R.J.; Weaver, S.; Hervé, F.; Larrondo, P. 1999. Mesozoic-Cenozoic evolution of the North Patagonian batholith in Aysen, southern Chile. *Journal of the Geological Society of London*, Vol. 156, p. 673-694.
- Scotese, C.R. 1997. Continental Drift flip book, 7<sup>th</sup> edition. Paleomap project. *University of Texas at Arlington, Department of Geology*, 79 p.
- Söllner, F.; Alfaro, G.; Miller, H. 2000. A Carboniferous/Permian metaigneimbrite from the coastal cordillera west of Puerto Montt, Los Lagos Region, Chile. In *Congreso Geológico Chileno*, No. 9, Actas, Vol. 2, p. 764-768. Puerto Varas.
- Tera, F.; Wasserburg, G. 1972. U-Th-Pb systematics in three Apollo 14 basalts and the problem of initial Pb in lunar rocks. *Earth and Planetary Science Letters*, Vol. 14, p. 281-304.
- Thomson, M.R.A. 1975. New palentological, and lithological observations on the Legoupil Formation, north-west Antarctic Peninsula. *British Antarctic Survey, Bulletin*, No. 41-42, p. 169-185.
- Thomson, S.N.; Hervé, F.; Fanning, C.M. 2000. Combining fission-track and U-Pb SHRIMP zircon ages to establish stratigraphic and metamorphic ages in basement sedimentary rocks in southern Chile. In *Congreso Geológico Chileno*, No. 9, Actas, Vol. 2, p. 769-773. Puerto Varas.
- Willan, R.C.R.; Pankhurst, R.J.; Hervé, F. 1994. A probable Early Triassic age for the Miers Bluff Formation, Livingston Island, South Shetland Islands. *Antarctic Science*, Vol. 6, No. 3, p. 401-408.
- Williams, I.S. 1998. U-Th-Pb geochronology by ion microprobe. In *Applications of microanalytical techniques to understanding mineralizing processes* (McKibben, M.A.; Shanks, W.C.; editors). *Reviews in Economic Geology*, Vol. 7, p. 1-35.
- Willner, A.; Hervé, F.; Massone, H.J. 2000. Mineral chemistry and pressure-temperature evolution of two contrasting high-pressure-low-temperature belts in the Chonos Archipelago, Southern Chile. *Journal of Petrology*, Vol. 41, No. 3, p. 309-330.

TABLE 1. SHRIMP U-Th-Pb RESULTS FOR ZIRCONS FROM SAMPLE CE9603.

Grain, spot	U (ppm)	Th (ppm)	Th/U (ppm)	Pb-2 (ppm)	<sup>206</sup> Pb/ <sup>238</sup> U I <sub>0</sub> <sup>206</sup>	Total ratios			Radiogenic Ratios			Ages (Ma) ± error (1 σ)			Conc. %				
						<sup>206</sup> Pb/ <sup>238</sup> U	<sup>207</sup> Pb/ <sup>235</sup> U	<sup>206</sup> Pb/ <sup>207</sup> Pb	<sup>206</sup> Pb/ <sup>238</sup> U	<sup>207</sup> Pb/ <sup>235</sup> U	<sup>206</sup> Pb/ <sup>207</sup> Pb	<sup>206</sup> Pb/ <sup>238</sup> U	<sup>207</sup> Pb/ <sup>235</sup> U	<sup>206</sup> Pb/ <sup>207</sup> Pb					
1.1	83	67	0.81	11	0.001712	2.07	16.18	0.51	0.0709	0.0026	0.0605	0.0019	379	12	1161	13	1134	20	104
2.1	188	488	2.59	20	0.000125	0.17	28.32	0.73	0.0522	0.0015	0.0353	0.0009	223	6	1014	25	1023	67	99
3.1	436	285	0.65	76	0.000988	0.12	11.78	0.19	0.0587	0.0013	0.0848	0.0014	525	8	1014	25	1023	67	99
4.1	696	193	0.28	90	0.003448	2.42	14.05	0.23	0.0750	0.0008	0.0694	0.0011	433	7	1014	25	1023	67	99
5.1	424	181	0.43	36	0.00579	0.48	22.74	0.37	0.0657	0.0011	0.0438	0.0007	276	4	1014	25	1023	67	99
6.1	91	28	0.30	32	0.000718	1.21	5.36	0.11	0.0865	0.0018	0.1842	0.0040	1090	22	1112	63	1156	178	94
7.1	412	269	0.65	32	0.001033	2.02	25.01	0.43	0.0673	0.0012	0.0392	0.0007	248	4	1014	25	1023	67	99
8.1	50	30	0.38	26	0.000282	0.48	5.41	0.18	0.0784	0.0017	0.1840	0.0062	1089	34	1077	40	1052	94	103
9.1	160	53	0.33	19	0.000692	0.30	15.74	0.33	0.0571	0.0014	0.0633	0.0013	396	8	1014	25	1023	67	99
10.1	734	397	0.54	93	0.000277	0.26	15.64	0.28	0.0668	0.0008	0.0638	0.0012	399	7	1014	25	1023	67	99
11.1	298	226	0.76	53	0.000432	0.38	12.00	0.34	0.0605	0.0021	0.0830	0.0024	514	14	1014	25	1023	67	99
12.1	230	130	0.55	39	0.000559	0.49	11.74	0.21	0.0617	0.0012	0.0848	0.0015	524	9	1014	25	1023	67	99
13.1	177	241	1.38	17	0.005195	1.83	25.03	0.57	0.0659	0.0037	0.0392	0.0009	248	6	1014	25	1023	67	99
14.1	183	238	1.30	16	0.004159	7.50	24.69	0.84	0.1112	0.0032	0.0375	0.0010	237	6	1014	25	1023	67	99
15.1	645	338	0.52	56	0.000386	0.13	22.87	0.30	0.0529	0.0008	0.0437	0.0005	276	4	1014	25	1023	67	99
16.1	130	73	0.55	12	0.000530	0.84	21.68	0.47	0.0586	0.0019	0.0480	0.0010	290	6	1014	25	1023	67	99
17.1	79	25	0.32	13	0.000435	0.88	11.68	0.36	0.0632	0.0033	0.0552	0.0026	527	16	1014	25	1023	67	99
18.1	652	820	1.24	112	0.000126	0.46	13.68	0.19	0.0597	0.0007	0.0729	0.0010	453	6	1014	25	1023	67	99
19.1	372	165	0.44	62	0.00079	0.13	11.65	0.16	0.0591	0.0008	0.0858	0.0012	530	7	1014	25	1023	67	99
20.1	296	55	0.27	24	0.000284	0.19	15.69	0.30	0.0552	0.0012	0.0636	0.0012	398	7	1014	25	1023	67	99
21.1	196	103	0.52	17	0.002063	4.13	22.48	0.42	0.0647	0.0019	0.0427	0.0008	259	5	1014	25	1023	67	99
22.1	75	23	0.30	12	0.001488	2.29	11.67	0.25	0.0754	0.0019	0.0837	0.0018	518	11	1014	25	1023	67	99
23.1	102	95	0.94	14	0.000276	0.78	15.38	0.37	0.0610	0.0033	0.0546	0.0016	404	10	1014	25	1023	67	99
24.1	53	44	0.70	11	0.000327	1.20	12.45	0.48	0.0657	0.0026	0.0734	0.0031	492	18	1014	25	1023	67	99
25.1	593	547	0.92	49	0.000010	0.15	25.45	0.42	0.0520	0.0009	0.0378	0.0006	239	4	1014	25	1023	67	99
26.1	368	133	0.56	67	0.000489	0.53	10.37	0.18	0.0540	0.0009	0.0359	0.0017	530	10	1014	25	1023	67	99
27.1	714	234	0.53	60	0.001174	0.80	22.67	0.35	0.0583	0.0012	0.0438	0.0007	276	4	1014	25	1023	67	99
28.1	552	151	0.27	21	0.000058	0.10	4.99	0.07	0.0783	0.0007	0.2002	0.0029	1176	16	1161	13	1134	20	104
29.1	128	51	0.40	17	0.000326	0.35	14.36	0.29	0.0593	0.0032	0.0594	0.0014	433	9	1014	25	1023	67	99
30.1	171	62	0.36	56	0.000421	0.72	5.66	0.10	0.0794	0.0035	0.1696	0.0030	1010	16	1014	25	1023	67	99
31.1	310	107	0.34	52	0.000769	0.51	11.29	0.25	0.0624	0.0012	0.0981	0.0020	544	12	1014	25	1023	67	99
32.1	115	159	1.38	9	1.86	29.47	0.85	0.0540	0.0035	0.0334	0.0010	212	5	1014	25	1023	67	99	
33.1	138	83	0.62	13	0.000882	0.70	20.85	0.48	0.0580	0.0018	0.0476	0.0011	300	7	934	22	959	57	96
34.1	169	70	0.42	51	0.000211	0.36	6.47	0.13	0.0741	0.0012	0.1539	0.0030	923	17	934	22	959	57	96
35.1	253	54	0.21	27	0.002389	1.18	16.61	0.34	0.0637	0.0024	0.0595	0.0012	373	7	934	22	959	57	96
36.1	111	81	0.73	9	0.003769	4.34	23.52	0.61	0.0961	0.0031	0.0407	0.0011	257	7	934	22	959	57	96
37.1	219	196	0.90	19	0.001762	0.39	25.90	0.45	0.0543	0.0016	0.0385	0.0007	243	4	934	22	959	57	96
38.1	987	352	0.36	79	0.000052	<0.01	23.45	0.29	0.0501	0.0007	0.0427	0.0005	270	3	934	22	959	57	96
39.1	400	202	0.50	126	0.000332	0.65	6.38	0.09	0.0730	0.0012	0.1567	0.0023	938	13	957	15	1001	38	94
40.1	1280	1134	1.24	220	0.000337	0.13	11.13	0.13	0.0595	0.0008	0.0897	0.0010	554	6	957	15	1001	38	94
41.1	188	109	0.58	19	0.000149	0.38	19.57	0.47	0.0558	0.0026	0.0509	0.0012	320	7	957	15	1001	38	94
42.1	215	68	0.32	31	0.000337	0.43	13.06	0.29	0.0571	0.0013	0.0765	0.0017	320	7	957	15	1001	38	94
43.1	582	585	0.85	62	0.000419	0.49	22.85	0.32	0.0558	0.0008	0.0439	0.0006	277	4	957	15	1001	38	94
44.1	782	401	0.51	45	0.000964	2.05	35.57	0.51	0.0665	0.0012	0.0292	0.0004	185	3	957	15	1001	38	94
45.1	254	87	0.34	32	0.001223	1.52	14.84	0.24	0.0672	0.0013	0.0664	0.0011	414	6	957	15	1001	38	94
46.1	486	82	0.17	47	0.000261	1.00	18.40	0.29	0.0616	0.0009	0.0538	0.0008	338	5	957	15	1001	38	94
47.1	403	195	0.48	26	0.001158	1.73	29.33	0.59	0.0646	0.0019	0.0335	0.0007	212	4	957	15	1001	38	94
48.1	558	25	0.05	78	0.000575	1.02	12.34	0.23	0.0652	0.0009	0.0602	0.0015	498	9	957	15	1001	38	94
49.1	71	15	0.22	7	0.012475	7.52	18.16	0.48	0.1132	0.0043	0.0509	0.0014	320	9	957	15	1001	38	94
50.1	507	24	0.05	72	0.012475	7.52	12.29	0.18	0.0593	0.0007	0.0611	0.0012	503	7	957	15	1001	38	94

Notes: 1- uncertainties given at the 1  $\sigma$  level; 2-  $f_{\text{Pb}}$  denotes the percentage of  $^{206}\text{Pb}$  that is common Pb; 3- For areas  $\geq 500$  Ma, correction for common Pb made using the measured  $^{206}\text{Pb}/^{238}\text{U}$  ratio; 4- For areas  $< 500$  Ma, correction for common Pb made using the measured  $^{206}\text{Pb}/^{238}\text{U}$  and  $^{207}\text{Pb}/^{235}\text{U}$  following Teri and Wasserburg (1972) as outlined in Compston *et al.* (1992); 5- For % Conc. -100% denotes a concordant analysis.

TABLE 2. SUMMARY OF SHRIMP U-Pb ZIRCON RESULTS FOR SAMPLE FO9606.

Grain, U spot (ppm)	Th (ppm)	Th/U (ppm)	Pb* (ppm)	$^{206}\text{Pb}/^{238}\text{Pb}$	$f_{\text{206}}$	Total ratios		Radiogenic ratios		Age (Ma) $\pm$ error (1 $\sigma$ )	Conc. %
						$^{206}\text{Pb}/^{238}\text{Pb}$	$^{207}\text{Pb}/^{235}\text{Pb}$	$^{206}\text{Pb}/^{238}\text{Pb}$	$^{207}\text{Pb}/^{235}\text{Pb}$	$^{206}\text{Pb}/^{238}\text{Pb}$	$^{207}\text{Pb}/^{235}\text{Pb}$
1.1	47	31	0.67	3	0.000136	0.72	0.0510	0.0053	0.0412	0.0013	260
2.1	150	108	0.22	28	0.000075	0.19	0.0825	0.0010	0.1115	0.0023	1411
3.1	437	304	0.61	56	0.000073	0.07	0.0882	0.0010	0.2447	0.0041	1411
4.1	137	94	0.62	56	0.000073	0.07	0.0882	0.0010	0.2447	0.0041	1411
5.1	238	116	1.56	27	0.000100	0.30	0.0519	0.0009	0.0442	0.0006	279
6.1	238	116	1.56	27	0.000100	0.30	0.0519	0.0009	0.0442	0.0006	279
7.1	334	160	0.52	19	0.000355	0.34	0.0213	0.0012	0.0468	0.0007	306
8.1	334	160	0.52	19	0.000355	0.34	0.0213	0.0012	0.0468	0.0007	306
9.1	240	103	0.43	16	0.000390	0.23	0.0520	0.0011	0.0443	0.0008	259
10.1	240	103	0.43	16	0.000390	0.23	0.0520	0.0011	0.0443	0.0008	259
11.1	159	124	0.62	18	0.000653	0.11	0.0527	0.0011	0.0448	0.0008	271
12.1	159	124	0.62	18	0.000653	0.11	0.0527	0.0011	0.0448	0.0008	271
13.1	129	20	0.63	13	0.000332	0.36	0.0546	0.0012	0.0564	0.0011	354
14.1	129	20	0.63	13	0.000332	0.36	0.0546	0.0012	0.0564	0.0011	354
15.1	237	116	0.42	22	0.000541	0.11	0.0523	0.0010	0.0461	0.0007	366
16.1	151	142	0.61	9	0.000100	0.17	0.0523	0.0010	0.0461	0.0007	366
17.1	81	64	0.80	7	0.000247	0.17	0.0523	0.0010	0.0461	0.0007	366
18.1	159	97	0.61	15	0.000375	0.29	0.0523	0.0010	0.0461	0.0007	366
19.1	279	100	0.36	20	0.000466	0.04	0.0527	0.0011	0.0463	0.0009	252
20.1	109	71	0.65	9	0.000326	0.33	0.0545	0.0018	0.0492	0.0010	310
21.1	54	43	0.79	4	0.000326	0.33	0.0545	0.0018	0.0492	0.0010	310
22.1	365	135	0.34	26	0.000157	0.17	0.0537	0.0009	0.0458	0.0006	280
23.1	365	135	0.34	26	0.000157	0.17	0.0537	0.0009	0.0458	0.0006	280
24.1	137	107	1.07	30	0.000010	0.44	0.0522	0.0009	0.0435	0.0006	274
25.1	137	107	1.07	30	0.000010	0.44	0.0522	0.0009	0.0435	0.0006	274
26.1	137	107	1.07	30	0.000010	0.44	0.0522	0.0009	0.0435	0.0006	274
27.1	137	107	1.07	30	0.000010	0.44	0.0522	0.0009	0.0435	0.0006	274
28.1	137	107	1.07	30	0.000010	0.44	0.0522	0.0009	0.0435	0.0006	274
29.1	137	107	1.07	30	0.000010	0.44	0.0522	0.0009	0.0435	0.0006	274
30.1	137	107	1.07	30	0.000010	0.44	0.0522	0.0009	0.0435	0.0006	274
31.1	204	76	0.37	17	0.000139	0.09	0.0545	0.0014	0.0551	0.0013	345
32.1	232	221	0.85	15	0.000010	0.01	0.0524	0.0015	0.0361	0.0008	229
33.1	386	281	0.73	31	0.000225	0.01	0.0519	0.0015	0.0469	0.0008	295
34.1	137	24	0.02	154	0.000659	0.13	0.0621	0.0005	0.0929	0.0013	573
35.1	365	257	0.70	23	0.000159	0.01	0.0523	0.0008	0.0380	0.0007	240
36.1	365	257	0.70	23	0.000159	0.01	0.0523	0.0008	0.0380	0.0007	240
37.1	237	380	0.54	26	0.000367	0.18	0.0523	0.0008	0.0415	0.0006	262
38.1	119	106	0.66	12	0.000200	0.28	0.0523	0.0008	0.0415	0.0006	262
39.1	119	106	0.66	12	0.000200	0.28	0.0523	0.0008	0.0415	0.0006	262
40.1	241	137	0.37	11	0.000010	0.66	0.0524	0.0013	0.0468	0.0013	216
41.1	410	129	0.31	22	0.000010	0.66	0.0524	0.0013	0.0468	0.0013	216
42.1	204	76	0.36	8	0.000010	0.66	0.0524	0.0013	0.0468	0.0013	216
43.1	177	64	0.36	7	0.000010	0.66	0.0524	0.0013	0.0468	0.0013	216
44.1	340	133	0.39	19	0.000658	0.01	0.0524	0.0013	0.0468	0.0013	216
45.1	497	228	0.48	20	0.000654	0.01	0.0524	0.0013	0.0468	0.0013	216
46.1	522	497	0.90	86	0.000121	0.78	0.0524	0.0013	0.0468	0.0013	216
47.1	522	497	0.90	86	0.000121	0.78	0.0524	0.0013	0.0468	0.0013	216
48.1	522	497	0.90	86	0.000121	0.78	0.0524	0.0013	0.0468	0.0013	216
49.1	177	62	0.36	7	0.000010	0.66	0.0524	0.0013	0.0468	0.0013	216
50.1	177	62	0.36	7	0.000010	0.66	0.0524	0.0013	0.0468	0.0013	216
51.1	960	55	0.06	134	0.000011	0.62	0.0524	0.0013	0.0468	0.0013	216
52.1	87	39	0.58	3	0.000011	0.62	0.0524	0.0013	0.0468	0.0013	216
53.1	426	91	0.21	17	0.000461	0.04	0.0524	0.0013	0.0468	0.0013	216
54.1	238	210	0.88	13	0.000010	0.66	0.0524	0.0013	0.0468	0.0013	216
55.1	605	42	0.07	29	0.000010	0.66	0.0524	0.0013	0.0468	0.0013	216
56.1	205	143	0.70	16	0.000010	0.66	0.0524	0.0013	0.0468	0.0013	216
57.1	174	107	0.61	13	0.002113	0.64	0.0524	0.0013	0.0468	0.0013	216
58.1	174	107	0.61	13	0.002113	0.64	0.0524	0.0013	0.0468	0.0013	216
59.1	174	107	0.61	13	0.002113	0.64	0.0524	0.0013	0.0468	0.0013	216
60.1	244	114	0.47	70	0.000668	0.01	0.0524	0.0013	0.0468	0.0013	216

Notes: 1. uncertainties given at the 1  $\sigma$  level. 2.  $f_{\text{206}}$  denotes the percentage of  $^{206}\text{Pb}$  that is common Pb. 3. for areas <800 Ma, correction for common Pb made using the measured  $^{206}\text{Pb}/^{238}\text{Pb}$  ratio. 4. for areas <800 Ma, correction for common Pb made using the measured  $^{207}\text{Pb}/^{235}\text{Pb}$  ratio. 5. For Conc. 100% denotes a concordant analysis.

TABLE 3. SUMMARY OF SHRIMP U-Pb ZIRCON RESULTS FOR SAMPLE CE9625

Grain spot	U (ppm)	Th (ppm)	Pb* (ppm)	Total ratios			Radiogenic ratios			Age (Ma) $\pm$ error (1 $\sigma$ )			Cont. %
				$^{206}\text{Pb}/^{238}\text{U}$	$^{207}\text{Pb}/^{235}\text{U}$	$^{206}\text{Pb}/^{207}\text{Pb}$	$^{206}\text{Pb}/^{238}\text{U}$	$^{207}\text{Pb}/^{235}\text{U}$	$^{206}\text{Pb}/^{207}\text{Pb}$	$^{206}\text{Pb}/^{238}\text{U}$	$^{207}\text{Pb}/^{235}\text{U}$	$^{206}\text{Pb}/^{207}\text{Pb}$	
1.1	680	331	0.49	0.000399	0.40	13.55	0.000399	0.0012	0.0044	0.0735	0.0012	0.0044	457
2.1	155	52	0.37	0.001318	2.35	17.43	0.001318	0.0026	0.0020	0.0560	0.0026	0.0020	351
3.1	317	212	0.67	0.000707	1.33	20.31	0.000707	0.0026	0.0020	0.0560	0.0026	0.0020	351
4.1	65	30	0.46	0.000154	1.36	9.45	0.000154	0.0011	0.0035	0.0480	0.0011	0.0035	305
5.1	367	174	0.47	0.001052	1.85	21.44	0.001052	0.0011	0.0035	0.0480	0.0011	0.0035	305
6.1	407	201	0.49	0.000525	4.20	21.35	0.000525	0.0011	0.0035	0.0480	0.0011	0.0035	289
7.1	241	39	0.16	0.000403	12.25	17.77	0.000403	0.0011	0.0035	0.0480	0.0011	0.0035	289
8.1	66	52	0.79	0.000049	0.01	5.84	0.000049	0.0011	0.0035	0.0480	0.0011	0.0035	289
9.1	94	28	0.30	0.000049	0.01	5.84	0.000049	0.0011	0.0035	0.0480	0.0011	0.0035	289
10.1	80	48	0.60	0.000049	0.01	5.84	0.000049	0.0011	0.0035	0.0480	0.0011	0.0035	289
11.1	337	156	0.39	0.000049	0.01	5.84	0.000049	0.0011	0.0035	0.0480	0.0011	0.0035	289
12.1	337	156	0.39	0.000049	0.01	5.84	0.000049	0.0011	0.0035	0.0480	0.0011	0.0035	289
13.1	167	172	0.43	0.001607	4.26	20.84	0.001607	0.0011	0.0035	0.0480	0.0011	0.0035	289
14.1	138	134	0.97	0.001997	2.61	30.24	0.001997	0.0011	0.0035	0.0480	0.0011	0.0035	289
15.1	185	140	0.85	0.001997	2.61	30.24	0.001997	0.0011	0.0035	0.0480	0.0011	0.0035	289
16.1	185	140	0.85	0.001997	2.61	30.24	0.001997	0.0011	0.0035	0.0480	0.0011	0.0035	289
17.1	333	131	0.39	0.000001	0.23	17.19	0.000001	0.0011	0.0035	0.0480	0.0011	0.0035	289
18.1	914	461	0.78	0.000282	1.58	21.68	0.000282	0.0011	0.0035	0.0480	0.0011	0.0035	289
19.1	115	111	0.96	0.000172	0.51	4.23	0.000172	0.0011	0.0035	0.0480	0.0011	0.0035	289
20.1	328	29	0.99	0.000349	0.87	10.77	0.000349	0.0011	0.0035	0.0480	0.0011	0.0035	289
21.1	123	184	1.26	0.000349	0.87	10.77	0.000349	0.0011	0.0035	0.0480	0.0011	0.0035	289
22.1	445	133	0.30	0.000262	0.23	15.97	0.000262	0.0011	0.0035	0.0480	0.0011	0.0035	289
23.1	762	203	0.37	0.000262	0.23	15.97	0.000262	0.0011	0.0035	0.0480	0.0011	0.0035	289
24.1	211	176	0.83	0.000262	0.23	15.97	0.000262	0.0011	0.0035	0.0480	0.0011	0.0035	289
25.1	172	127	0.74	0.000422	0.51	10.87	0.000422	0.0011	0.0035	0.0480	0.0011	0.0035	289
26.1	64	28	0.44	0.000422	0.51	10.87	0.000422	0.0011	0.0035	0.0480	0.0011	0.0035	289
27.1	49	28	0.58	0.000422	0.51	10.87	0.000422	0.0011	0.0035	0.0480	0.0011	0.0035	289
28.1	259	48	0.19	0.000014	<0.01	3.20	0.000014	0.0011	0.0035	0.0480	0.0011	0.0035	289
29.1	113	84	0.75	0.000349	0.87	10.77	0.000349	0.0011	0.0035	0.0480	0.0011	0.0035	289
30.1	297	258	0.87	0.000349	0.87	10.77	0.000349	0.0011	0.0035	0.0480	0.0011	0.0035	289
31.1	172	180	0.76	0.000349	0.87	10.77	0.000349	0.0011	0.0035	0.0480	0.0011	0.0035	289
32.1	196	165	0.53	0.000010	0.01	6.39	0.000010	0.0011	0.0035	0.0480	0.0011	0.0035	289
33.1	636	95	0.15	0.000010	0.01	6.39	0.000010	0.0011	0.0035	0.0480	0.0011	0.0035	289
34.1	184	68	0.37	0.000010	0.01	6.39	0.000010	0.0011	0.0035	0.0480	0.0011	0.0035	289
35.1	479	273	1.08	0.000010	0.01	6.39	0.000010	0.0011	0.0035	0.0480	0.0011	0.0035	289
36.1	115	97	0.84	0.000010	0.01	6.39	0.000010	0.0011	0.0035	0.0480	0.0011	0.0035	289
37.1	43	6	0.15	0.000010	0.01	6.39	0.000010	0.0011	0.0035	0.0480	0.0011	0.0035	289
38.1	51	15	0.63	0.000010	0.01	6.39	0.000010	0.0011	0.0035	0.0480	0.0011	0.0035	289
39.1	85	54	0.80	0.000010	0.01	6.39	0.000010	0.0011	0.0035	0.0480	0.0011	0.0035	289
40.1	301	76	0.32	0.000010	0.01	6.39	0.000010	0.0011	0.0035	0.0480	0.0011	0.0035	289
41.1	750	286	0.38	0.000010	0.01	6.39	0.000010	0.0011	0.0035	0.0480	0.0011	0.0035	289
42.1	390	201	0.51	0.000010	0.01	6.39	0.000010	0.0011	0.0035	0.0480	0.0011	0.0035	289
43.1	245	127	0.52	0.000010	0.01	6.39	0.000010	0.0011	0.0035	0.0480	0.0011	0.0035	289
44.1	393	526	1.34	0.000010	0.01	6.39	0.000010	0.0011	0.0035	0.0480	0.0011	0.0035	289
45.1	354	209	0.59	0.000010	0.01	6.39	0.000010	0.0011	0.0035	0.0480	0.0011	0.0035	289

Notes: 1-; uncorrected as given at the 1  $\sigma$  level; 2-;  $f_{\text{cor}}$  % denotes the percentage of  $^{206}\text{Pb}$  that is common Pb; 3-; for areas  $<800$  Ma, correction for common Pb made using the measured  $^{206}\text{Pb}/^{207}\text{Pb}$  ratio; 4-; for areas  $<800$  Ma, correction for common Pb made using the measured  $^{206}\text{Pb}/^{207}\text{Pb}$  following Tera and Wasserburg (1972) as outlined in Compton et al. (1992); 5-; for % Cont., 100% denotes a concordant analysis.

TABLE 4. SUMMARY OF SHRIMP U-Pb ZIRCON RESULTS FOR SAMPLE F06540.

Grain spot	U (ppm)	Th (ppm)	Th/U	Pb* (ppm)	$^{206}\text{Pb}/^{238}\text{Pb}$	$f_{\text{206}}$	Radiogenic ratios				Ages (Ma) $\pm$ error (1 $\sigma$ )				Conc. %
							$^{206}\text{Pb}/^{238}\text{Pb}$	$\pm$	$^{206}\text{Pb}/^{235}\text{Pb}$	$\pm$	$^{206}\text{Pb}/^{238}\text{Pb}$	$\pm$	$^{207}\text{Pb}/^{235}\text{Pb}$	$\pm$	
1.1	76	59	0.78	15	0.001103	0.23	0.1164	0.0025	1.844	0.032	0.0743	0.0007	710	15	102
2.1	489	48	0.10	128	0.000032	<0.01	0.1830	0.0004					1067	13	102
3.1	1324	30	0.02	265	0.000000	<0.01	0.1415	0.0017					553	18	100
4.1	435	379	0.87	43	0.000032	0.65	0.0570	0.0003					2041	22	100
5.1	1235	266	1.63	23	0.000032	0.65	0.0570	0.0003	6.429	0.038	0.1252	0.0010	2032	14	100
6.1	1235	266	1.63	23	0.000032	0.65	0.0570	0.0003					2032	14	100
7.1	210	103	0.49	129	0.000032	0.03	0.3737	0.0004	5.882	0.194	0.1142	0.0030	1867	48	110
8.1	207	263	0.68	82	0.000077	0.13	0.1630	0.0025	1.628	0.041	0.0724	0.0013	981	29	98
9.1	207	263	0.68	82	0.000077	0.13	0.1630	0.0025	6.050	0.143	0.1198	0.0010	1953	14	104
10.1	115	40	0.35	34	0.000072	0.11	0.3887	0.0078	1.970	0.072	0.0752	0.0023	1121	17	104
11.1	1217	63	0.05	186	0.000064	0.60	0.1991	0.0012					667	7	104
12.1	749	90	0.12	126	0.000035	<0.01	0.1164	0.0014					710	8	104
13.1	435	614	1.41	66	0.000082	0.03	0.0777	0.0010					552	10	104
14.1	120	107	0.89	23	0.000446	0.10	0.0572	0.0013					461	11	104
15.1	260	168	0.60	74	0.000189	<0.01	0.1932	0.0003	1.827	0.078	0.0721	0.0025	1087	21	110
16.1	151	105	0.42	59	0.000337	0.06	0.1932	0.0003	1.753	0.041	0.0726	0.0010	1058	17	106
17.1	134	17	0.13	20	0.005754	11.75	0.1932	0.0003					541	13	102
18.1	97	33	0.34	13	0.000166	0.32	0.1932	0.0003	6.825	0.190	0.1278	0.0022	2111	32	102
19.1	85	38	0.45	54	0.000217	0.31	0.3874	0.0069					552	9	102
20.1	223	324	1.45	39	0.000217	0.31	0.3874	0.0069					552	9	102
21.1	46	35	0.77	11	0.002862	2.30	0.1467	0.0047					883	27	97
22.1	176	329	0.42	158	0.000010	0.30	0.1709	0.0017	1.761	0.003	0.0743	0.0004	1031	8	97
23.1	1135	545	0.48	314	0.000032	0.05	0.1719	0.0019					1031	8	97
24.1	113	106	0.94	6	0.000513	0.24	0.0837	0.0053	2.170	0.044	0.0812	0.0010	1142	16	93
25.1	130	45	1.05	42	0.000065	<0.01	0.0973	0.0028					359	5	93
26.1	224	45	1.05	42	0.000065	<0.01	0.0973	0.0028					359	5	93
27.1	756	459	0.69	113	0.000010	0.01	0.0898	0.0015					555	9	93
28.1	125	55	0.44	25	0.000054	1.14	0.1244	0.0024					555	9	93
29.1	156	163	1.05	31	0.000201	0.27	0.1097	0.0025					871	15	93
30.1	482	391	0.81	63	0.000010	<0.01	0.0754	0.0011					469	6	93
31.1	34.1	445	0.10	53	0.000031	<0.01	0.0831	0.0011	1.834	0.040	0.0738	0.0011	514	7	103
32.1	281	158	0.56	24	0.000036	0.02	0.1501	0.0026					1068	14	103
33.1	281	158	0.56	24	0.000036	0.02	0.1501	0.0026					1068	14	103
34.1	311	110	0.35	87	0.000010	<0.01	0.0535	0.0008					365	8	96
35.1	311	110	0.35	87	0.000010	<0.01	0.0535	0.0008					365	8	96
36.1	311	110	0.35	87	0.000010	<0.01	0.0535	0.0008					365	8	96
37.1	146	198	0.70	53	0.000113	0.18	0.3024	0.0051	4.546	0.105	0.1090	0.0015	1703	25	96
38.1	120	50	0.40	34	0.000242	0.43	0.1922	0.0029	1.736	0.068	0.0731	0.0022	1024	20	101
39.1	120	50	0.40	34	0.000242	0.43	0.1922	0.0029	2.041	0.125	0.0778	0.0045	1123	15	99
40.1	152	99	0.35	49	0.000297	<0.01	0.1903	0.0029					653	14	104
41.1	157	35	0.23	25	0.000297	0.10	0.1066	0.0025	19.32	0.40	0.2245	0.0015	3127	47	104
42.1	91	75	0.82	108	0.000044	0.06	0.6242	0.0119					704	10	99
43.1	358	157	0.44	65	0.000029	<0.01	0.0903	0.0015					557	9	99
44.1	208	119	0.57	31	0.000073	0.12	0.2116	0.0036	2.400	0.085	0.0823	0.0016	1237	19	99
45.1	215	98	0.45	73	0.000139	0.12	0.0578	0.0007					537	4	99
46.1	648	306	0.47	59	0.000033	<0.01	0.0893	0.0021					537	4	99
47.1	548	62	0.11	98	0.000033	<0.01	0.0893	0.0021	1.631	0.043	0.0724	0.0014	982	17	98
48.1	158	67	0.62	100	0.000169	0.22	0.4779	0.0165	11.29	0.28	0.1713	0.0017	2518	46	98
49.1	352	67	0.62	100	0.000169	0.22	0.4779	0.0165					560	10	98
50.1	352	67	0.62	100	0.000169	0.22	0.4779	0.0165					560	10	98
51.1	311	246	0.44	60	0.000024	0.08	0.1077	0.0018					587	9	98
52.1	647	229	0.35	56	0.000010	0.02	0.0943	0.0015					587	9	98
53.1	567	264	0.47	51	0.000082	0.22	0.0876	0.0017					541	10	92
54.1	347	141	0.41	28	0.000112	0.32	0.0876	0.0017					541	10	92
55.1	314	160	0.51	47	0.000112	0.21	0.1588	0.0031	1.611	0.047	0.0736	0.0014	950	17	92

Notes: 1- uncertainties given at the 1  $\sigma$  level; 2-  $f_{\text{206}}$  % denotes the percentage of  $^{206}\text{Pb}$  that is common Pb; 3- for areas >800 Ma, correction for common Pb made using the measured  $^{206}\text{Pb}/^{238}\text{Pb}$  ratio; 4- for areas <800 Ma, correction for common Pb made using the measured  $^{207}\text{Pb}/^{235}\text{Pb}$  and  $^{206}\text{Pb}/^{238}\text{Pb}$  following Terrell and Wasserburg (1972) as outlined in Compagnon et al. (1992); 5- for % Conc. 100% denotes a concordant analysis.